DOI 10.1007/s11204-016-9356-x
Soil Mechanics and Foundation Engineering, Vol. 53, No. 1, March, 2016 (Russian Original No. 1, January-February, 2016)

STRENGTH AND DEFORMABILITY OF CLAY SOIL UNDER DIFFERENT TRIAXIAL LOAD REGIMES THAT CONSIDER CRACK FORMATION

I. T. Mirsayapov and I. V. Koroleva
Kazan' State University of Architecture and Engineering, Kazan', Tatarstan.

UDC 624.131.439.6

A spatial model of dilatating soil under triaxial load conditions with different regimes are described on the basis of a hypothesis that the Coulomb dry friction force acts in the plane of tangential particle shear. Spatial soil deformation over time is described in accordance with the theory of inherited creep in the form of the sum of deformations due to changes in volume and shape, with due regard for their interrelation.

Introduction

Existing methods of analyzing beds in terms of bearing capacity and deformations have been developed primarily for cases of single, short-duration static loading or cyclical loading with cycle parameters that remain constant over the entire operating period.

Under actual conditions, loads are applied to soil beds in stages, as the building or structure is erected. Here, stages of active loading during construction transition to stages of long-term reaction to load if the building contains no equipment that creates dynamic loads or of if such equipment is installed in the building, there are stages of successive alternation of long-term static and cyclical loads. Actual (realistic) loading schemes for soil beds are shown in Fig. 1.

There is a need to refine the method for analyzing the bearing capacity and settlement of foundations for actual regimes of long-term static and cyclic loading. This task is particularly important for beds composed of clay soil, since in this case the stress-deformation state varies over time and depends on the prior loading history.

General mathematical models are proposed in [1-6], describing deformation and failure behaviors in clay soil under arbitrary loading regimes and paths, although no recommendations are provided for their practical implementation.

The plasticity theory laws used to develop analytical models are not capable of duly considering the influence of such factors as dilatancy, crack formation and development, reinforcement, reduction in internal friction angle, and specific cohesion, volumetric deformation modulus, and shear modulus for different loading regimes.

In this regard, experiments were carried out on clay soil under triaxial load conditions for the regimes shown in Fig. 1.

Translated from Osnovaniya, Fundamenty i Mekhanika Gruntov, No. 1, pp. 5-10, January-February, 2016.
0038-0741/16/5301-0005

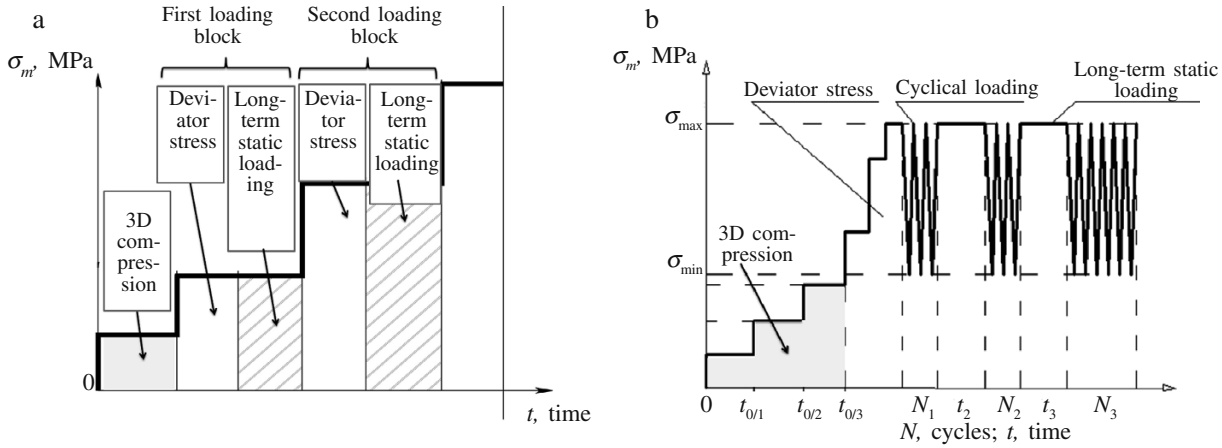

Fig. 1. Actual regimes: a) long-term static loading; b) long-term cyclical loading.

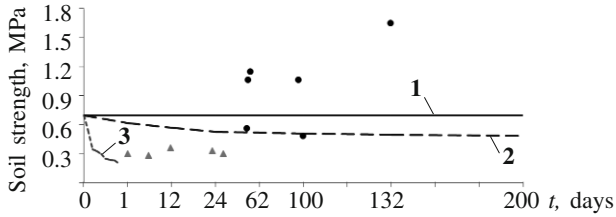

Fig. 2. Change in soil strength in response to different loading regimes: 1) single short-duration static loading; 2) long-term static loading; 3) short-term cyclical loading; •) long-term static regime loading; ▵) long-term cyclical regime loading.

Experimental study results

As follows from Figs. 2 and 3, all axial parameters-deformation modulus, shear modulus, specific cohesion, internal friction angle, and ultimate stress-undergo changes in the examined regimes that describe the stressed and deformed state of soil over time, which permits the conclusion that it is impossible to select some constant for their value for a specific soil. The analytical models must include functional dependencies to calculate these parameters for different loading regimes.

Analytical model of soil deformation

Based on the results of experiments and the data in [7-9], it is assumed that for triaxial loading of a specimen, staged increases in load result in compressed zones in the form of pyramids of different size and shape, depending on the loading regime (Fig. 4). Deformation of a specimen occurs as a result of the motion of these pyramids as solid bodies. The physical and mechanical properties of soil do not degrade in compressed zones, but improve (density, φ, and c increase). Negative processes that reduce soil characteristics, are localized in a zone between the "pyramids" and the soil in this zone is simultaneously subject to cleavage and shear.

Based on the results in [1-10], we represent volumetric deformation in the form

$$\varepsilon_v(t,\tau)=\varepsilon_{v,0}(t_1,\tau)\pm\sum_{i=1}^{n}\varepsilon_{v,D_i}(t_2,\tau)\pm\sum_{j=1}^{m}\varepsilon_{v,D_j}^{\max}(t_3,\tau), \quad (1)$$

where $\varepsilon_{v,0}(t_1, \tau)$ is the volumetric deformation for three-dimensional compression, $\varepsilon_{v,D_i}(t_2, \tau)$ and $\varepsilon_{v,D_j}^{\max}(t_3,\tau)$ are the volumetric deformations caused by a stress deviator; n and m are, respectively, the stages of deviator loading and exposure at maximum load, or cyclical loading.

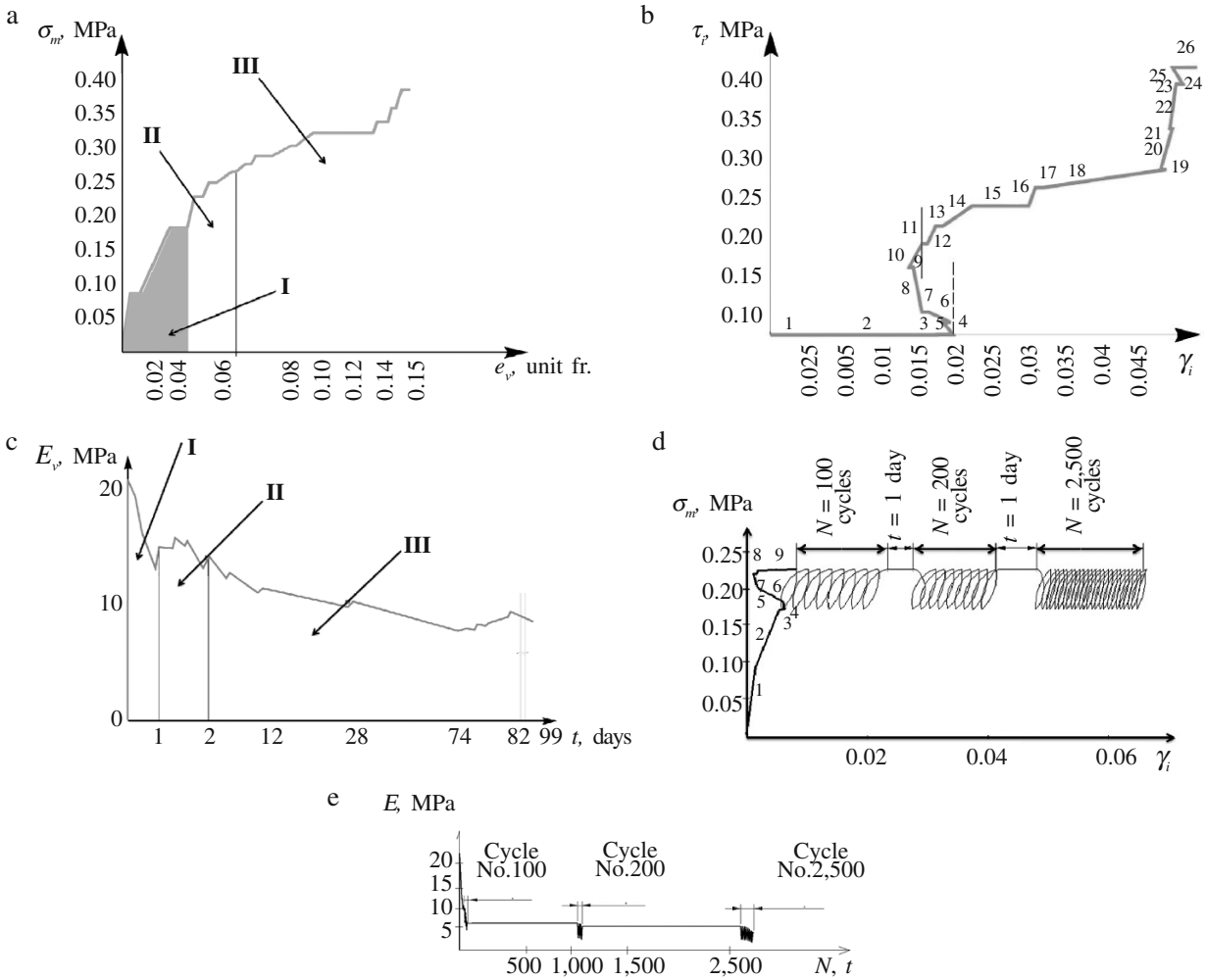

Fig. 3. Experimental study results: σ_m is the average stress; *ev* is the volumetric deformation; τ_i is the tangential stress; γ_i is the shear deformation intensity; E_v is the volumetric deformation modulus; *t* is time; I is three-dimensional compression (stages 1-4); II is deviator stress (stages 4-11); III is block deviator static and long-term loading (stages 11-26).

Soil deformation over time is described in accordance with the Boltzmann-Volterra theory of inherited creep modified by Maslov-Arutyunyan. Complete shear or volume deformation under an arbitrary loading regime:

$$\varepsilon_i(t,\tau)=\frac{\sigma_i(t)}{G(t)}+\frac{1}{G(t)}\int_\tau^t K_\gamma(t,\tau)\sigma_i(\tau)d\tau, \tag{2}$$

$$\varepsilon_{v,D_j}^{\max}(t_3,\tau)=\frac{\sigma(t)}{K(t)}+\frac{1}{K(t)}\int_\tau^t K_V(t,\tau)\sigma(\tau)d\tau, \tag{3}$$

where $G(t)$ and $K(t)$ are shear modulus and volumetric deformation variables, $K_\gamma(t, \tau)$ and $K_V(t, \tau)$ are creep kernels that represent the rate of shear and volumetric deformation for unit load intensities and average stress (taken per [5]).

Based on the model [5] and the results of experiments, a scheme is proposed for inelastic deformation of clay soil, in which the Coulomb dry friction force deviates from the limit equilibrium area element and acts in a plane of purely tangential particle shear. Determining the orientation of potentially hazardous area elements requires consideration of the deformed state of the soil.

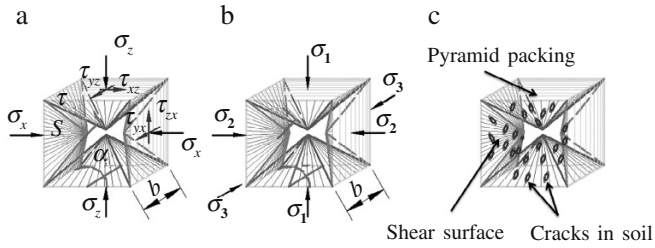

Fig. 4. Stressed state in a unit volume of soil in X, Y, Z, space at an arbitrary time t in a pre-limit state (a); in the principal stress state at the stage of limit equilibrium (b); diagram of crack development in limit equilibrium planes within a unit volume of soil (c).

Retaining the principle of stress and deformation rate tensor coaxiality [5], we assume that the Coulomb dry friction force law links the projections of forces acting on limit equilibrium area elements on the normal to the shear area element and the area element itself. Then the flow condition for long-term loading:

$$|t| = S\tan\varphi(t,t_1,N,\tau) + c_0(t,t_1,N,\tau), \tag{4}$$

where $S = \sigma_1 ll' + \sigma_2 mm' + \sigma_3 nn'$; $t = ((\sigma_1 lm' - \sigma_2 ml')^2 + + (\sigma_2 mn' - \sigma_3 nm')^2 + (\sigma_3 nl' - \sigma_1 ln')^2)^{1/2}$; $\varphi(t, t_1, N, \tau)$ and $c_0(t, t_1, N, \tau)$ are the time-dependent internal friction angle and specific cohesion variables; l, m, n, l', m', and n' are the direction cosines of the normals to the limit equilibrium and shear area element s, respectively.

The spatial orientation of the limit equilibrium area elements varies during inelastic soil deformation in response to regime loading and is taken in accordance with [5].

Based on the stated model and the results of research (see Figs. 2 and 3), the strength conditions for triaxial compression:

$$4[\sigma_V(t,t_1,N)A_{sh}\cos\alpha_1(t,t_1,N) + \tau_V(t,t_1,N)A_{sh}\sin\alpha_1(t,t_1,N)] \geq \sigma_1 A_1, \tag{5}$$

where $A_{sh} = b^2/(4\cos\alpha_2(t, t_1, N))$ is the surface area of the lateral sides of a pyramid; $A_1 = b^2$ is the area of the sides of a cube; $.\alpha_1(t, t_1, N)$ and $\alpha_2(t, t_1, N)$ are time-dependent variables of the angle of inclination of the limit equilibrium and shear area element; $\sigma_v(t, t_1, N)=\sigma_1 l(t, t_1, N)l'(t, t_1, N)+\sigma_2 m(t, t_1, N)m'(t, t_1, N) + + \sigma_3 n(t, t_1, N)n'(t, t_1, N)+\sigma_d(t, t_1, N)$ are the normal stresses; $\sigma_d(t, t_1, N) = E\Delta\delta_d/((1 + \nu)r)$ are the dilatant stresses; $\tau_V(t, t_1, N)=S\tan\varphi_0(t, t_1, N, \tau) + c_0(t, t_1, N, \tau)$ are the tangential stresses in the limit equilibrium area element.

Thus, soil strength in response to triaxial compression depends on the varying angle of internal friction, the specific cohesion, and the angle of inclination of the limit equilibrium plane.

Per the results of [1, 2, 5], failure occurs when the extent of damage from microcracks in the limit equilibrium zone attains a critical value. Soil strength is reduced over time, principally, by reduced cohesion forces, while at the same time, the internal friction angle changes little.

Relying on the results of [3-6], we proposal the following scheme for development of creep deformations and changes in long-term strength during the loading process. Depending on the magnitude and duration of a load in clay soil, there occur two oppositely directed processes-reinforcement, caused by rebonding of defects and more dense rearrangement of particles, and degradation, caused by the reorientation of particles and the formation and propagation of micro- and macrocracks (Fig. 4). A stage of failure and progressive creep occurs in those cases where degradation starts to prevail over reinforcement. An intense disruption of microstructures and reorientation of particles occurs in this stage; moreover, these processes do not encompass the entire volume of soil, but only zones of limit equilibrium with reduced strength, where cracks develop (see Fig. 4).

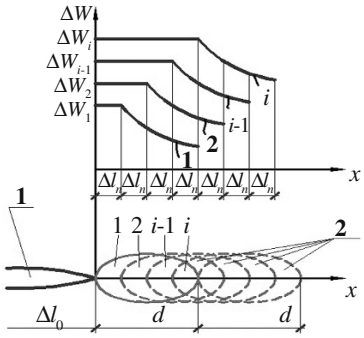

Fig. 5. Diagram of shear crack development in limit equilibrium planes: 1) macro-/microcrack; 2) zones of plastic soil deformation.

The crack development process may, for convenience, be divided into three stages. The first stage is that of soil disintegration, which starts with the appearance of submicroscopic cracks. Cracks appear at pores or at the continuations of shrinkage microcracks (structural defects).

At this stage, cracks are small and it is more correct to speak of the formation of local plastically deformed sections that unite a set of sub-microcracks and gradually form a disintegration chain that prepares a route for microcracks. At the initial stage of loading, several disintegration zones are formed, distributed throughout the entire volume. The disintegration chains turn into microcracks only if a certain concentration of sub-microcracks is achieved. Large-sized microcracks or macrocracks are formed as the load exposure time or number of loading cycles increases in the zones where deformation energy is sufficient to unite individual increments of disintegrated soil.

This stage may be called the incubation stage. The higher the load, the shorter this stage.

The second stage begins when one of the microcracks, which finds itself under the most adverse conditions, becomes a macrocrack. A zone of plastically deformed material (disintegration zone) always forms along the front of a developing macrocrack, and subsequent crack growth occurs as a result of this terminal zone. Processes of material disintegration in the terminal plastic zone and new macrocrack section creation alternate. Then, depending on the level of stress, the macrocrack develops via stable or stepwise progress along the length of the disintegration zone. Subsequently, this process repeats systematically.

The second stage ends when the macrocrack achieves a critical size. The crack then develops in an unstable manner by means of the energy of deformation of the analyzed soil volume.

The duration of the third stage is normally negligible in comparison to the previous stages, and it manifests itself on the descending leg of the soil deformation diagram. The transition between stages is stepwise.

The critical opening of the crack tip

$$\delta(x,\ t,\ l) = \delta_{cr} \tag{6}$$

is taken to be the "failure" criterion (the beginning of increase in length).

The growth in the crack length occurs in a stepwise manner by Δl_n as stresses increase, until an overall length d is attained (Fig. 5).

The start of macrocrack development follows. Here, it is assumed that cracks develop in stages as deformations at the tip achieve a critical value. The increased crack length Δl_n (see Fig. 5) at each stage is determined from the condition:

$$\sum\left[\Delta W_i - \Delta W_r\left(\frac{\Delta W_i}{W_r}\right)^{\beta}\right] = \text{const} = W_{pl}. \tag{7}$$

The stress intensity factor at the crack tip is:

$$K_{\mathrm{I}cf}(t)=\sqrt{E_p J_{cf}(t)},\quad K_{\mathrm{II}cf}(t)=\sqrt{G_p J_{cf}(t)}. \tag{8}$$

The contour interval is:

$$J_{cf}(t)=\sqrt{2E_p\left(\int\limits_0^{\varepsilon_R}\sigma_{t_R}d\varepsilon-\int\limits_0^{\varepsilon_{mp}-\varepsilon_{pl}}\sigma_{t_i}d\varepsilon\right)}\frac{k_0^2 R_{so}k_{fb}d_s}{E_{so,t}}. \tag{9}$$

The energy accumulated within the plastic deformation zone at the crack tip is:

$$\Delta W_{i_{(i-1)}}=\frac{1}{\sqrt{2\pi\left[d+(i-1)\Delta l_{n_i}\right]}}\left\{\begin{array}{l}\left[K_{\mathrm{I}_{cf}}(t)\varphi_{11}(\sigma)+K_{\mathrm{II}_{cf}}(t)\varphi_{21}(\sigma)\right]^2-\\-\left[c_e a\psi_v\prod\limits_{k=1}^{k=j}K_k+\sum\limits_{n=2}^{N_{i-1}}c_e\prod\limits_{k=1}^{k=j}K_k(1-a\psi_v)^{N_{i-1}-1}a\psi_{v_i}\right]\end{array}\right\}. \tag{10}$$

The overall crack length in the soil is:

$$l(t,\tau)=l(t_0)+l_{pl}(t,\tau), \tag{11}$$

where $l(t_0)$ is the initial crack length at the stage of microcrack development; $l_{pl}(t,\tau)=\sum\limits_{i=1}^{n}\Delta l_n$ is the crack length that depends on plastic deformations.

The above equations are valid provided cracks are situated sufficiently far from each other, i.e., when their interaction may be ignored. It is known that the interaction of micro- and macrocracks may result in a reduction or increase in soil deformability and strength, depending on the mutual positions of the microcracks and their orientation.

One of the most effective methods of addressing the issue of micro- and macrocrack interaction is the method of singular integral equations [11]. The essence of the method reduces to the construction of a complex potential using the superposition method.

The mutual influence is considered by increasing the stress intensity factor at the tip of the macrocrack [11]:

$$K_I(t,N)=\pm\lim_{x_n\to l_n}\sqrt{\frac{l_n^2-x_n^2}{l_n}}g'_n(x), \tag{12}$$

where $g'n(x)$ are the derivatives of displacement discontinuities for the k-th crack; $l(n)$ is the length of the n-th crack; x_n is the coordinate of the point under consideration.

The derivative of the displacement discontinuity at the tip of the macrocrack, with due regard for the formation of a system of micro- and macrocracks in the soil of the analyzed volume is [11]:

$$g'n(x) = (B/B_0)g'_{n0}(x), \tag{13}$$

where B and B_0 are functions of the yielding property of the soil massif when a system of cracks is present (B) or when there is one crack in the volume under consideration (B_0).

The expression that takes account of the change in specific cohesion between soil particles has the general form:

$$c_0(t,\ \tau) = K^{\mathrm{M}}_{\mathrm{I}ct}q(S), \tag{14}$$

where $q(S)$ is a function of the total crack length S; $K^{\mathrm{M}}_{\mathrm{I}ct}$ is the factor of stress intensity at the crack tip during the loading process.

Hereinafter, using the method in [5], after performing certain transformations and simplifications, we obtain the soil strength reduction function:

$$\eta(t,\tau_1)=m(t,\tau_1)\lambda(t,\tau_1)\sqrt{\frac{K(\tau_1)}{K(t)}\frac{1}{1+K(\tau_1)C(t,\tau_1)}}. \tag{15}$$

Then the specific cohesion between particles is, with due regard for the time factor:

$$C_0(t,\tau_1)=C_0(\tau_1)m(t,\tau_1)\lambda\left(t,\tau_1\right)\sqrt{\frac{K(\tau_1)}{K(t)}\frac{1}{1+K(\tau_1)C(t,\tau_1)}}, \tag{16}$$

where $C(t,\ \tau_1)$ is the measure of volumetric soil creep; $C_0(\tau_1)$ is the initial specific cohesion of soil for short-term loading; $m(t,\ \tau_1)$ is a function of soil reinforcement due to the restoration of water-colloidal bonds; $\lambda(t,\ \tau_1)$ is a function of reinforcement due to the restoration of structural bonds in the soil, with due regard for the mixture of different blocks during the loading process.

The functions $m(t,\ \tau_1)$ and $\lambda(t,\ \tau_1)$ consider delay effects in crack propagation, self-reinforcement, and self-rebonding of clay soil via the restoration of structure and coagulational bonds.

The change in the soil internal friction angle is determined by the changes in orientation of limit equilibrium area elements over long-term inelastic deformation.

Conclusion

Analytical models have been developed for the deformation and strength of clay soil under different triaxial loading regimes, including expressions to determine the specific cohesion and internal friction angle, as well as shear moduli and linear and volumetric deformations.

Analytical models correctly reflect features of nonlinear deformation in clay soil.

REFERENCES

1. S. S. Vyalov, *Rheological Fundamentals of Soil Mechanics* [in Russian], Vysshaya shkola, Moscow (1978).
2. S. S. Vyalov, N. K. Pekarskaya, and R.V. Maksimyak, "Physical essence of processes of deformation and failure of clayey soils," *Osn. Fundam. Mekh. Gruntov*, No. 1, 7-9 (1970).
3. Yu. K. Zaretskii, *Soil Viscosity and Plasticity and Structural Analysis* [in Russian], Stroiizdat, Moscow (1988).
4. Yu. K. Zaretskii, "Long-term strength and viscoplasticity of clay soil," *Osn. Fundam. Mekh. Gruntov*, No. 2, 2-6 (1995).
5. Yu. K. Zaretskii and S. S. Vyalov, "Structural mechanics of clay soils," *Osn. Fundam. Mekh. Gruntov*, No. 3, 2-12 (1971).
6. V. N. Razbegin, "Viscoplasticity of ice and certain types of soils," *Osn. Fundam. Mekh. Gruntov*, No. 6, 2-9 (1995).
7. I. T. Mirsayapov and I. V. Koroleva, "Prediction of deformations of foundation beds with a consideration of long-term nonlinear soil deformation," *Osn. Fundam. Mekh. Gruntov*, No. 4, 16-23 (2011).
8. I. T. Mirsayapov, I. V. Koroleva, and O. A. Ivanova, "Low-cycle fatigue life and deformation of clayey soil under triaxial cyclical loading," *Zhilishchnoe stroitel'stvo*, No. 9, 6-8 (2012).
9. I. T. Mirsayapov and I. V. Koroleva, "Analytical model for long-term non-linear deformation of clayey soil in a complex loaded state," *Izv. KGASU*, No. 2 (16), 121-128 (2011).
10. I. T. Mirsayapov and I. V. Koroleva, "Aspects of deformation of clayey soil under performance loading," *Izv. KGASU*, No. 4 (22), 193-198 (2012).
11. V. V. Panasyuk, M. P. Savruk, and A. P. Datsyshin, Stress distribution near a fracture in thin plates and shells," *Naukova Dumka*, Kiev (1976).